

The macroscale boundary conditions for diffusion in a material with microscale varying diffusivities

Chen Chen¹A. J. Roberts²J. E. Bunder³

(Received 19 December 2013; revised 5 June 2014; corrected 1 August 2014)

Abstract

Homogenization and other multiscale modelling techniques empower us to build efficient mathematical models for simulating materials with complicated microstructures. However, the modelling rarely systematically derives boundary conditions for the macroscale models. We build a smooth macroscale model for a two-layer one-dimensional lattice diffusion system with rapidly varying diffusivity and finite scale separation. We derive macroscale boundary conditions for this diffusion problem. Our approach is applicable to a range of multiscale modelling problems including wave equations.

<http://journal.austms.org.au/ojs/index.php/ANZIAMJ/article/view/7853> gives this article, © Austral. Mathematical Soc. 2014. Published August 1, 2014, as part of the Proceedings of the 11th Biennial Engineering Mathematics and Applications Conference. ISSN 1446-8735. (Print two pages per sheet of paper.) Copies of this article must not be made otherwise available on the internet; instead link directly to this URL for this article.

Contents

1	Introduction	C219
2	Centre manifold theory determines macroscopic model	C223
2.1	First iteration to construct centre manifold model	C225
2.2	More iterations give more accuracy	C227
3	Spatial evolution gives accurate boundary conditions	C227
3.1	Spatial evolution mapping \mathbb{T}	C227
3.2	Macroscopic boundary conditions at $x = 0$	C229
3.3	Macroscopic boundary conditions at $x = L$	C231
4	Result and conclusion	C232

1 Introduction

We model and analyse diffusion in a microstructured two-layer one-dimensional metamaterial of length L . The microstructure is defined by rapidly varying diffusivity, both across and between the layers. The aim is to derive correct boundary conditions for the macroscale continuum model of the diffusion.

Figure 1 shows the diffusion system on the microscale lattice with varying diffusivity. The microscale differential equations for the ‘temperature’ $u_{n,j}(t)$ at time t , layer $j = 0, 1$ and lateral node $n = 1, 2, \dots, N - 1$ are

$$h^2 \frac{du_{n,0}}{dt} = a_{n-1,0}(u_{n-1,0} - u_{n,0}) + a_{n,0}(u_{n+1,0} - u_{n,0}) + a_n(u_{n,1} - u_{n,0}),$$

$$h^2 \frac{du_{n,1}}{dt} = a_{n-1,1}(u_{n-1,1} - u_{n,1}) + a_{n,1}(u_{n+1,1} - u_{n,1}) + a_n(u_{n,0} - u_{n,1}), \quad (1)$$

with microscale lattice spacing $h = L/N$. Dirichlet boundary conditions define the temperature at the four endpoints of the material: $u_{0,j}$ and $u_{N,j}$ for $j = 0, 1$. The diffusivities $a_{n,j}$ and a_n define the microstructure and

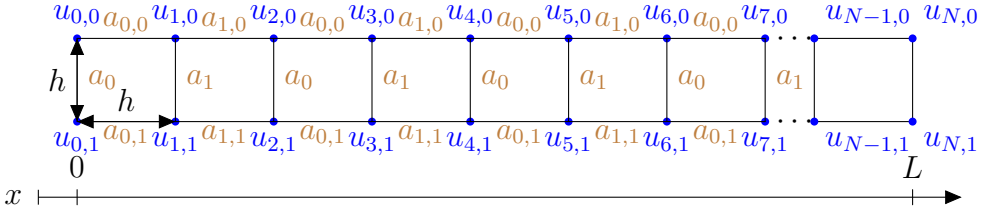


Figure 1: Model a microstructured material of length L defined on a lattice with microscale lattice spacing h ; the variable diffusion has a lateral periodicity of two: $\mathbf{a}_{l,j}$ and \mathbf{a}_l for $l = 0, 1$ along a layer and $j = 0, 1$ between layers; ‘temperature’ $u_{n,j}(t)$ varies in time and is defined at each lattice node $\mathbf{n} = 0, 1, \dots, N$ and $j = 0, 1$.

are constant between each node but vary with periodicity two in the lateral index \mathbf{n} , that is, for even \mathbf{n} , $\mathbf{a}_{n,j} = \mathbf{a}_{0,j}$ and $\mathbf{a}_n = \mathbf{a}_0$, and for odd \mathbf{n} , $\mathbf{a}_{n,j} = \mathbf{a}_{1,j}$ and $\mathbf{a}_n = \mathbf{a}_1$. The diffusivities are also different in different layers $j = 0, 1$. Therefore, we have a total of six different diffusivities.

The diffusion system (1) simulates heat transfer in a metamaterial. Metamaterials are artificial materials designed to have special properties that may not be found in nature. Metamaterials are typically constructed from a periodic arrangement of two or more microscopic materials with distinctly different properties. For example, engineers manipulate the microstructure of metamaterials so that they have negative permittivity and permeability and thus a negative index of refraction (Eleftheriades and Selvanayagam, 2012; Dong and Itoh, 2012). The diffusion system (1), illustrated in Figure 1, is a metamaterial composed of alternating microscopic materials with distinctly different diffusion properties. Macroscale modelling techniques which are able to predict properties of proposed metamaterials enhance their research significantly because manufacturing even a small amount of metamaterial can be very expensive (Baron et al., 2013; Mei and Vernescu, 2010).

In the engineering of a metamaterial we are interested in its macroscale dynamics rather than its microscopic response. Specifically, we are not

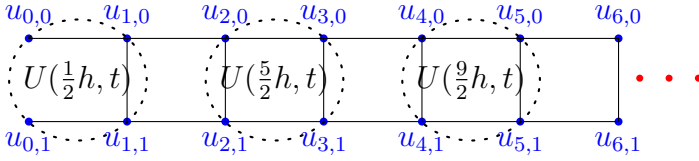


Figure 2: The macroscopic temperature $\mathbf{U}(x, t)$ is defined as an average over one period of the microscale temperature.

interested in the details of the diffusion between layers $j = 0, 1$ and at each $n = 0, 1, \dots, N$, but desire a model which describes the lateral diffusion over a scale larger than the microscale lattice spacing h . So we must derive a macroscale model for the diffusion system (1). Section 2 applies centre manifold theory (Mercer and Roberts, 1990; Roberts, 2011) which, from the microscale lattice diffusion system (1), determines the macroscale homogenised diffusion PDE

$$\frac{\partial \mathbf{U}}{\partial t} \approx \mathbf{A} \frac{\partial^2 \mathbf{U}}{\partial x^2}, \quad (2)$$

where constant \mathbf{A} is an effective diffusivity and $\mathbf{U}(x, t)$ is the macroscale local mean temperature of the material along the lateral dimension x .

Figure 2 illustrates the definition of the macroscale temperature as an average of microscale temperatures:

$$\mathbf{U}(x, t) := (\mathbf{u}_{2n,1} + \mathbf{u}_{2n+1,1} + \mathbf{u}_{2n,0} + \mathbf{u}_{2n+1,0})/4 \quad \text{at } x = (2n + \frac{1}{2})h, \quad (3)$$

where here, $n = 0, 1, \dots, (N - 1)/2$. Section 3 derives macroscale boundary conditions in the Robin form $\mathbf{U} + w_4 \frac{\partial \mathbf{U}}{\partial x} = \mathbf{C}$, for constant w_4 and \mathbf{C} , at $x = 0, L$ for the macroscale model (2). The derivation proceeds by considering the spatial evolution when moving away from either boundary into the interior (Roberts, 1992). Figure 3 shows that our boundary conditions with the macroscale model (2) give excellent agreement with the microscale simulation. In contrast, the commonly used classic boundary conditions perform poorly.

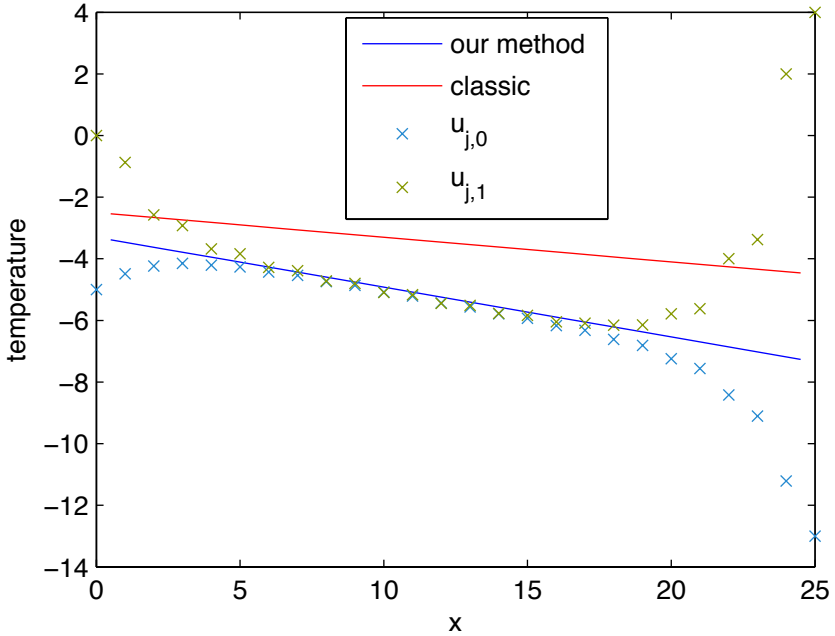


Figure 3: The blue crosses are the microscale temperatures $u_{n,0}$ in the top layer and the green crosses are those in the bottom layer, $u_{n,1}$. These microscale temperatures are from the steady state analytical solution of diffusion equation (1). The difference between the blue and green crosses at the two ends are boundary layers of the diffusion system. The blue line is our macroscale model (2) obtained using boundary conditions (22) that correctly produce the interior solution. The red line is the macroscale model obtained with classic boundary values.

2 Centre manifold theory determines macroscopic model

The first aim is to develop a macroscale diffusion PDE (2) using centre manifold theory. Each circle in Figure 2 captures one full period of the microscale system. We call this repetitive unit a cell. We seek solutions in the form of a Fourier transform

$$\mathbf{u}_{n,j}(\mathbf{t}) = \int_{-\pi/2}^{\pi/2} \tilde{\mathbf{u}}_{l,j}(\mathbf{k}, \mathbf{t}) e^{i\mathbf{k}h\mathbf{n}} d\mathbf{k} \quad \text{for } l = n \bmod 2,$$

where $l = 0, 1$, and $j = 0, 1$, and \mathbf{k} denotes a lateral wavenumber relative to the microscale lattice spacing. The subscripts l and j split a potentially ‘spiky’ temperature $\mathbf{u}_{n,0}(\mathbf{t})$ and $\mathbf{u}_{n,1}(\mathbf{t})$ into four ‘smooth’ temperature functions: $\tilde{\mathbf{u}}_{0,0}(\mathbf{k}, \mathbf{t})$ represents the temperature in the Fourier domain at the top left node of a cell; and $\tilde{\mathbf{u}}_{1,0}(\mathbf{k}, \mathbf{t})$, $\tilde{\mathbf{u}}_{0,1}(\mathbf{k}, \mathbf{t})$ and $\tilde{\mathbf{u}}_{1,1}(\mathbf{k}, \mathbf{t})$ represent the same, but at the top right, bottom left and bottom right nodes of a cell, respectively. This splitting allow us to see the slowly varying nature of the microscale diffusion (1).

In Fourier variables the diffusion problem is now

$$\begin{aligned} h^2 \frac{d\tilde{\mathbf{u}}_{0,0}}{dt} &= \mathbf{a}_{1,0}(\tilde{\mathbf{u}}_{1,0} e^{-i\mathbf{h}\mathbf{k}} - \tilde{\mathbf{u}}_{0,0}) + \mathbf{a}_{0,0}(\tilde{\mathbf{u}}_{1,0} e^{i\mathbf{h}\mathbf{k}} - \tilde{\mathbf{u}}_{0,0}) + \mathbf{a}_0(\tilde{\mathbf{u}}_{0,1} - \tilde{\mathbf{u}}_{0,0}), \\ h^2 \frac{d\tilde{\mathbf{u}}_{0,1}}{dt} &= \mathbf{a}_{1,1}(\tilde{\mathbf{u}}_{1,1} e^{-i\mathbf{h}\mathbf{k}} - \tilde{\mathbf{u}}_{0,1}) + \mathbf{a}_{0,1}(\tilde{\mathbf{u}}_{1,1} e^{i\mathbf{h}\mathbf{k}} - \tilde{\mathbf{u}}_{0,1}) + \mathbf{a}_0(\tilde{\mathbf{u}}_{0,0} - \tilde{\mathbf{u}}_{0,1}), \\ h^2 \frac{d\tilde{\mathbf{u}}_{1,0}}{dt} &= \mathbf{a}_{0,0}(\tilde{\mathbf{u}}_{0,0} e^{-i\mathbf{h}\mathbf{k}} - \tilde{\mathbf{u}}_{1,0}) + \mathbf{a}_{1,0}(\tilde{\mathbf{u}}_{0,0} e^{i\mathbf{h}\mathbf{k}} - \tilde{\mathbf{u}}_{1,0}) + \mathbf{a}_1(\tilde{\mathbf{u}}_{1,1} - \tilde{\mathbf{u}}_{1,0}), \\ h^2 \frac{d\tilde{\mathbf{u}}_{1,1}}{dt} &= \mathbf{a}_{0,1}(\tilde{\mathbf{u}}_{0,1} e^{-i\mathbf{h}\mathbf{k}} - \tilde{\mathbf{u}}_{1,1}) + \mathbf{a}_{1,1}(\tilde{\mathbf{u}}_{0,1} e^{i\mathbf{h}\mathbf{k}} - \tilde{\mathbf{u}}_{1,1}) + \mathbf{a}_1(\tilde{\mathbf{u}}_{1,0} - \tilde{\mathbf{u}}_{1,1}). \end{aligned} \quad (4)$$

Write the system (4) in matrix vector form by defining $\vec{\mathbf{u}} := (\tilde{\mathbf{u}}_{0,0}, \tilde{\mathbf{u}}_{0,1}, \tilde{\mathbf{u}}_{1,0}, \tilde{\mathbf{u}}_{1,1})$:

$$h^2 \frac{d\vec{\mathbf{u}}}{dt} = \mathcal{L}_{\mathbf{k}} \vec{\mathbf{u}}, \quad (5)$$

where

$$\mathcal{L}_k := \begin{bmatrix} -a_{1,0} - a_{0,0} - a_0 & a_0 & 0 & 0 \\ a_0 & -a_{1,1} - a_{0,1} - a_0 & 0 & 0 \\ 0 & 0 & -a_{0,0} - a_{1,0} - a_1 & a_1 \\ 0 & 0 & a_1 & -a_{0,1} - a_{1,1} - a_1 \end{bmatrix} + e^{-i\mathbf{h}\mathbf{k}} \begin{bmatrix} 0 & 0 & a_{1,0} & 0 \\ 0 & 0 & 0 & a_{1,1} \\ a_{0,0} & 0 & 0 & 0 \\ 0 & a_{0,1} & 0 & 0 \end{bmatrix} + e^{i\mathbf{h}\mathbf{k}} \begin{bmatrix} 0 & 0 & a_{0,0} & 0 \\ 0 & 0 & 0 & a_{0,1} \\ a_{1,0} & 0 & 0 & 0 \\ 0 & a_{1,1} & 0 & 0 \end{bmatrix}.$$

A useful subspace of equilibria for the system (4) is the wavenumber $\mathbf{k} = \mathbf{0}$ and all temperatures identical $\tilde{\mathbf{u}}_{0,0} = \tilde{\mathbf{u}}_{0,1} = \tilde{\mathbf{u}}_{1,0} = \tilde{\mathbf{u}}_{1,1}$. Let $\mathcal{L}_0 = \mathcal{L}_k|_{\mathbf{k}=\mathbf{0}}$. The matrix \mathcal{L}_0 has an eigenvalue of zero, and the corresponding eigenvector is $(1, 1, 1, 1)$ (using the Strang notation that parentheses denote the corresponding column vector). Because matrix \mathcal{L}_0 is symmetric, all eigenvalues are real. Let λ be any eigenvalue corresponding to some eigenvector $\vec{\mathbf{v}} = (v_1, v_2, v_3, v_4)$ which is not $(1, 1, 1, 1)$. Because the matrix \mathcal{L}_0 is real

$$\begin{aligned} \lambda |\vec{\mathbf{v}}|^2 &= \vec{\mathbf{v}}^T \lambda \vec{\mathbf{v}} = \vec{\mathbf{v}}^T \mathcal{L}_0 \vec{\mathbf{v}} \\ &= -a_0 (v_1 - v_2)^2 - a_1 (v_3 - v_4)^2 \\ &\quad - (a_{1,1} + a_{0,1}) (v_2 - v_4)^2 - (a_{0,0} + a_{1,0}) (v_1 - v_3)^2 \\ &< 0. \end{aligned}$$

Hence, any eigenvalue corresponding to an eigenvector other than $(1, 1, 1, 1)$ is real and negative. The strict inequality is because $\vec{\mathbf{v}}$ cannot be a multiple of $(1, 1, 1, 1)$. Then centre manifold theory assures us of the existence, relevance and approximation of a slow manifold macroscale model in a finite neighbourhood of the equilibria $\vec{\mathbf{u}} \propto (1, 1, 1, 1)$ and wavenumber $\mathbf{k} = \mathbf{0}$ (Carr and Muncaster, 1983; Roberts, 2011).

Since the equilibria all have wavenumber $\mathbf{k} = \mathbf{0}$, the neighbourhood of validity includes all small wavenumbers \mathbf{k} , which correspond to solutions slowly varying in space \mathbf{x} . Since the equilibria form a subspace, spanned by $(1, 1, 1, 1)$, the model is global in macroscale amplitude \mathbf{U} . The macroscale model is parametrised by any reasonable chosen measure of amplitude in each cell (Carr, 1982). We choose the amplitude to satisfy (3) in each cell.

2.1 First iteration to construct centre manifold model

The next step is to construct the centre manifold as a power series in wavenumber k . Use the Taylor series expansion $e^{\pm i\hbar k} = 1 \pm i\hbar k - \frac{1}{2}\hbar^2 k^2 + \mathcal{O}(k^3)$. Rewrite the ODEs (5) as

$$\frac{d\vec{u}}{dt} = \mathcal{L}_0 \frac{\vec{u}}{\hbar^2} + \begin{bmatrix} 0 & 0 & \delta_{0,0} & 0 \\ 0 & 0 & 0 & \delta_{0,1} \\ \delta_{1,0} & 0 & 0 & 0 \\ 0 & \delta_{1,1} & 0 & 0 \end{bmatrix} \frac{\vec{u}}{\hbar^2} + \mathcal{O}(k^3), \quad (6)$$

where

$$\delta_{l,j} = \mathbf{a}_{1-l,j} \left(-i\hbar k - \frac{1}{2}\hbar^2 k^2 \right) + \mathbf{a}_{l,j} \left(i\hbar k - \frac{1}{2}\hbar^2 k^2 \right).$$

Define the m th residual of the dynamical system equation (6) to be

$$\text{Res}^{[m]} := \frac{d\vec{u}^{[m-1]}}{dt} - \mathcal{L}_0 \frac{\vec{u}^{[m-1]}}{\hbar^2} - \begin{bmatrix} 0 & 0 & \delta_{0,0} & 0 \\ 0 & 0 & 0 & \delta_{0,1} \\ \delta_{1,0} & 0 & 0 & 0 \\ 0 & \delta_{1,1} & 0 & 0 \end{bmatrix} \frac{\vec{u}^{[m-1]}}{\hbar^2},$$

where $\vec{u}^{[m-1]}$ is the m th approximation of \vec{u} . Substitute the initial approximation, $\vec{u}^{[0]} = \tilde{\mathbf{U}}(1, 1, 1, 1)$ such that $\frac{d\tilde{\mathbf{U}}}{dt} \approx \mathbf{g}^{[0]} = 0$, to calculate the first residual

$$\text{Res}^{[1]} = -\frac{\tilde{\mathbf{U}}}{\hbar^2} \begin{bmatrix} \mathbf{a}_{1,0} \left(-i\hbar k - \frac{1}{2}\hbar^2 k^2 \right) + \mathbf{a}_{0,0} \left(i\hbar k - \frac{1}{2}\hbar^2 k^2 \right) \\ \mathbf{a}_{1,1} \left(-i\hbar k - \frac{1}{2}\hbar^2 k^2 \right) + \mathbf{a}_{0,1} \left(i\hbar k - \frac{1}{2}\hbar^2 k^2 \right) \\ \mathbf{a}_{0,0} \left(-i\hbar k - \frac{1}{2}\hbar^2 k^2 \right) + \mathbf{a}_{1,0} \left(i\hbar k - \frac{1}{2}\hbar^2 k^2 \right) \\ \mathbf{a}_{0,1} \left(-i\hbar k - \frac{1}{2}\hbar^2 k^2 \right) + \mathbf{a}_{1,1} \left(i\hbar k - \frac{1}{2}\hbar^2 k^2 \right) \end{bmatrix} + \mathcal{O}(k^3). \quad (7)$$

We seek corrections, indicated by hats, to the approximations $\vec{u}^{[m]}$ and $\mathbf{g}^{[m]}$ to give the next approximations:

$$\vec{u}^{[m+1]} := \vec{u}^{[m]} + \hat{\vec{u}}, \quad \mathbf{g}^{[m+1]} := \mathbf{g}^{[m]} + \hat{\mathbf{g}}. \quad (8)$$

Substitute (8) and initial approximations $\vec{u}^{[0]}$ and $g^{[0]}$ into (6) to compute the update rule

$$\text{Res}^{[m]} = \mathcal{L}_0 \hat{u} - \mathcal{E} \hat{g}, \tag{9}$$

where $\mathcal{E} := (1, 1, 1, 1)$. Since matrix \mathcal{L}_0 is symmetric, \mathcal{E} is also the left eigenvector corresponding to the zero eigenvalue. Premultiply (9) by \mathcal{E}^T with residual (7) to find the solvability condition:

$$-\frac{\tilde{U}}{h^2} (-\alpha_{1,0} h^2 k^2 - \alpha_{0,0} h^2 k^2 - \alpha_{1,1} h^2 k^2 - \alpha_{0,1} h^2 k^2) = -4\hat{g}.$$

Thus this first iteration yields the effective diffusivity as the arithmetic average of the four lateral diffusivities (modified in the next iteration)

$$\frac{d\tilde{U}}{dt} \approx g^{[1]} = -\frac{(\alpha_{0,0} + \alpha_{0,1} + \alpha_{1,0} + \alpha_{1,1}) k^2}{4} \tilde{U}. \tag{10}$$

Now substitute evolution (10) into the update equation (9) with the known first residual $\text{Res}^{[1]}$ to compute \hat{u} . The system of equations is deficient so we need one more equation to find \hat{u} . From the amplitude definition (3), adjoin the amplitude condition $\hat{u}_{1,1} + \hat{u}_{0,0} + \hat{u}_{0,1} + \hat{u}_{1,0} = 0$, to solve

$$\begin{bmatrix} \mathcal{L}_0 \\ \vec{1}^T \end{bmatrix} \hat{u} = \frac{k\tilde{U}}{h} \begin{bmatrix} \alpha_{1,0} \left(i + \frac{1}{4}hk\right) + \alpha_{0,0} \left(-i + \frac{1}{4}hk\right) - (\alpha_{0,1} + \alpha_{1,1})hk/4 \\ \alpha_{1,1} \left(i + \frac{1}{4}hk\right) + \alpha_{0,1} \left(-i + \frac{1}{4}hk\right) - (\alpha_{1,0} + \alpha_{0,0})hk/4 \\ \alpha_{0,0} \left(i + \frac{1}{4}hk\right) + \alpha_{1,0} \left(-i + \frac{1}{4}hk\right) - (\alpha_{1,0} + \alpha_{1,1})hk/4 \\ \alpha_{0,1} \left(i + \frac{1}{4}hk\right) + \alpha_{1,1} \left(-i + \frac{1}{4}hk\right) - (\alpha_{1,0} + \alpha_{0,0})hk/4 \\ 0 \end{bmatrix}. \tag{11}$$

Solve the system of equations (11) by QR factorisation for \hat{u} and hence find $\vec{u}^{[1]}$.

Knowing $\vec{u}^{[1]}$ and $g^{[1]}$, we compute the second residual $\text{Res}^{[2]}$. The second residual is $\mathcal{O}(k^2)$ which indicates $\vec{u}^{[1]}$ has errors $\mathcal{O}(k^2)$.

2.2 More iterations give more accuracy

Knowing the second residual $\text{Res}^{[2]}$ is $\mathcal{O}(k^2)$, we now compute corrections of $\mathcal{O}(k^2)$. Following the same procedure as in Section 2.1 one more iteration gives the more accurate evolution

$$\frac{d\tilde{u}}{dt} \approx -k^2 \mathcal{A} \tilde{u}, \quad (12)$$

where the effective macroscale diffusion coefficient is

$$\mathcal{A} = \frac{\mathbf{a}_0 \mathbf{a}_1 (\mathbf{a}_{01} + \mathbf{a}_{00}) (\mathbf{a}_{11} + \mathbf{a}_{10}) + (\mathbf{a}_0 + \mathbf{a}_1) \sum_{j=0}^1 \sum_{l=0}^1 \mathbf{a}_{0,0} \mathbf{a}_{0,1} \mathbf{a}_{1,0} \mathbf{a}_{1,1} / \mathbf{a}_{l,j}}{\mathbf{a}_1 \mathbf{a}_0 (\mathbf{a}_{0,0} + \mathbf{a}_{0,1} + \mathbf{a}_{1,0} + \mathbf{a}_{1,1}) + (\mathbf{a}_1 + \mathbf{a}_0) (\mathbf{a}_{1,1} + \mathbf{a}_{0,1}) (\mathbf{a}_{1,0} + \mathbf{a}_{0,0})}.$$

The inverse Fourier transform of the evolution equation (12) gives the macroscale diffusion PDE (2).

The evolution (12) has errors $\mathcal{O}(k^4)$. We could apply more iterations to derive a higher order model but will not do so here.

3 Spatial evolution gives accurate boundary conditions

This section derives boundary conditions for the macroscale diffusion PDE (2). We define the temperature's spatial structure, evolving across the spatial domain, similarly to the evolving time-like variable described by Roberts (1992).

3.1 Spatial evolution mapping \mathbb{T}

The aim here is to derive the spatial mapping \mathbb{T} shown schematically in Figure 4. Then spatial boundary layers will be accounted for in the 'dynamics'

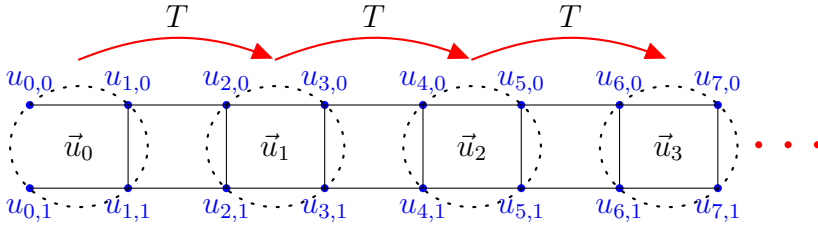


Figure 4: At equilibrium, spatial structures are determined by the map T from cell to adjacent cell. The map T is invariant across the domain because of the choice of a unit cell and the periodicity of the problem.

of the map T . We are primarily interested in the long lasting, slowly-varying modes as away from the boundaries the solution in the interior is slowly varying—for example, the interior region of Figure 3. For slow spatial modes, without much loss in accuracy, assume the time derivative term in equation (1) is negligible: numerical experiments indicate this neglect is effective. Nontrivial initial values are subject to future research. The lattice diffusion system (1) simplifies to algebraic equations. These algebraic equations connect eight nodes within any two adjacent cells:

$$\begin{aligned}
 0 &= a_{n-1,0}(\mathbf{u}_{n-1,0} - \mathbf{u}_{n,0}) + a_{n,0}(\mathbf{u}_{n+1,0} - \mathbf{u}_{n,0}) + a_n(\mathbf{u}_{n,1} - \mathbf{u}_{n,0}), \\
 0 &= a_{n-1,1}(\mathbf{u}_{n-1,1} - \mathbf{u}_{n,1}) + a_{n,1}(\mathbf{u}_{n+1,1} - \mathbf{u}_{n,1}) + a_n(\mathbf{u}_{n,0} - \mathbf{u}_{n,1}), \\
 0 &= a_{n,0}(\mathbf{u}_{n,0} - \mathbf{u}_{n+1,0}) + a_{n-1,0}(\mathbf{u}_{n+2,0} - \mathbf{u}_{n+1,0}) + a_{n-1}(\mathbf{u}_{n+1,1} - \mathbf{u}_{n+1,0}), \\
 0 &= a_{n,1}(\mathbf{u}_{n,1} - \mathbf{u}_{n+1,1}) + a_{n-1,1}(\mathbf{u}_{n+2,1} - \mathbf{u}_{n+1,1}) + a_{n-1}(\mathbf{u}_{n+1,0} - \mathbf{u}_{n+1,1}), \quad (13)
 \end{aligned}$$

where the first cell contains $\mathbf{u}_{n-1,j}$ and $\mathbf{u}_{n,j}$ and the second cell contains $\mathbf{u}_{n+1,j}$ and $\mathbf{u}_{n+2,j}$, both with $j = 0, 1$. Rearrange the homogeneous linear system (13) into a 4×4 inhomogeneous system

$$T \begin{bmatrix} \mathbf{u}_{n-1,0} \\ \mathbf{u}_{n-1,1} \\ \mathbf{u}_{n,0} \\ \mathbf{u}_{n,1} \end{bmatrix} = \begin{bmatrix} \mathbf{u}_{n+1,0} \\ \mathbf{u}_{n+1,1} \\ \mathbf{u}_{n+2,0} \\ \mathbf{u}_{n+2,1} \end{bmatrix}.$$

This determines the spatial evolution map T shown in Figure 4. Let $\vec{v}_1, \vec{v}_2, \vec{v}_3$ and \vec{v}_4 be the four eigenvectors of the spatial map T and μ_1, μ_2, μ_3 and μ_4 be the corresponding eigenvalues. For all microscale diffusivities $\alpha_{n,j}$, the spatial mapping T always has two eigenvalues of 1 and two eigenvalues with a product of 1. Let $\mu_2 = \mu_3 = 1$, and let $\mu_1 < 1 < \mu_4$. As the matrix T is not diagonalisable, let v_3 be the generalised eigenvector satisfying $(T - I)\vec{v}_3 = \vec{v}_2$. To justify the eigenspectrum, the eigenvector $\vec{v}_2 = (1, 1, 1, 1)$ and generalised genvector $\vec{v}_3 = (1, 1, -1, -1)$ corresponding to two eigenvalues of 1 are independent of the diffusivities. Furthermore, the determinant of mapping T is one so the product of all four eigenvalues is one and hence $\mu_1\mu_4 = 1$. Assuming all diffusivities are physical and positive, μ_1 and μ_4 are real and $\mu_1 < 1 < \mu_4$.

Write the first cell $\vec{u}_0 = (u_{0,0}, u_{0,1}, u_{1,0}, u_{1,1})$ as a linear combinations of the eigenvectors,

$$\vec{u}_0 = c_1\vec{v}_1 + c_2\vec{v}_2 + c_3\vec{v}_3 + c_4\vec{v}_4, \tag{14}$$

for some coefficients c_p where $p \in \{1, 2, 3, 4\}$, and where the first two components of the vector (14), $u_{0,0}$ and $u_{0,1}$, are the left end boundary values. The microscale solution in the n th cell $\vec{u}_n = (u_{2n,0}, u_{2n,1}, u_{2n+1,0}, u_{2n+1,1})$ is then

$$\vec{u}_n = T^n\vec{u}_0 = c_1\mu_1^n\vec{v}_1 + c_2\vec{v}_2 + c_3(\vec{v}_3 + n\vec{v}_2) + c_4\mu_4^n\vec{v}_4. \tag{15}$$

3.2 Macroscopic boundary conditions at $x = 0$

We derive the left macroscale boundary condition from the mapping T . At the left end the coefficient $c_4 = 0$ because if $c_4 \neq 0$, then the growing mode $c_4\mu_4^n\vec{v}_4$ would generate a exponentially large value at the right end of the domain. So the general quasi-equilibrium solution of system (1) near the left end is

$$\vec{u}_n = c_1\mu_1^n\vec{v}_1 + c_2\vec{v}_2 + c_3(\vec{v}_3 + n\vec{v}_2). \tag{16}$$

The prescribed boundary values are the first two components of the cell \vec{u}_0 ,

$$\begin{aligned} u_{0,0} &= c_1v_{11} + c_2v_{21} + c_3v_{31}, \\ u_{0,1} &= c_1v_{12} + c_2v_{22} + c_3v_{32}. \end{aligned} \tag{17}$$

Recall that equation (3) defined the macroscale temperature at the n th cell as the arithmetic average of the microscale temperatures in the n th cell, $\mathbf{u}_{2n,0}$, $\mathbf{u}_{2n,1}$, $\mathbf{u}_{2n+1,0}$ and $\mathbf{u}_{2n+1,1}$. Within the interior of the domain of the microscale system (1) μ_1^n is negligible (as $\mu_1 < 1$) so

$$\mathbf{U}(x = 2nh + 0.5h) = \frac{1}{4}\vec{\mathbf{u}}_n \cdot \vec{\mathbf{1}} = \frac{c_2}{4}\vec{\mathbf{v}}_2 \cdot \vec{\mathbf{1}} + \frac{c_3}{4}(\vec{\mathbf{v}}_3 + n\vec{\mathbf{v}}_2) \cdot \vec{\mathbf{1}}.$$

Therefore, the macroscale spatial derivative determined from linear interpolation is

$$\frac{\partial \mathbf{U}}{\partial x} = \frac{\mathbf{U}(x = 2nh + 2.5h) - \mathbf{U}(x = 2nh + 0.5h)}{2h} = \frac{c_3\vec{\mathbf{v}}_2}{8h} \cdot \vec{\mathbf{1}}. \quad (18)$$

Extrapolation from the domain interior back through the boundary layer towards the left end then estimates \mathbf{U} on the left boundary:

$$\begin{aligned} \mathbf{U}(x = 0) &= \mathbf{U}(x = 2nh + 0.5h) - (2nh + 0.5h) \frac{\partial \mathbf{U}}{\partial x} \\ &= \frac{1}{4} [c_2\vec{\mathbf{v}}_2 + c_3(\vec{\mathbf{v}}_3 - \frac{1}{4}\vec{\mathbf{v}}_2)] \cdot \vec{\mathbf{1}}. \end{aligned} \quad (19)$$

Adjoin macroscopic equations (18) and (19) to the microscale boundary conditions (17), then using $\vec{\mathbf{v}}_2 = \vec{\mathbf{1}}$ we obtain

$$\begin{bmatrix} v_{11} & 1 & v_{31} \\ v_{12} & 1 & v_{32} \\ 0 & 1 & \frac{1}{4}(\vec{\mathbf{v}}_3 \cdot \vec{\mathbf{1}} - 1) \\ 0 & 0 & \frac{1}{8h}\vec{\mathbf{v}}_2 \cdot \vec{\mathbf{1}} \end{bmatrix} \begin{bmatrix} c_1 \\ c_2 \\ c_3 \end{bmatrix} = \begin{bmatrix} \mathbf{u}_{0,0} \\ \mathbf{u}_{0,1} \\ \mathbf{U}|_{x=0} \\ \frac{\partial \mathbf{U}}{\partial x}|_{x=0} \end{bmatrix}. \quad (20)$$

System (20) defines four equations with three unknowns and is solvable when the RHS is in the range of the LHS matrix. Ensuring the RHS is in the range provides a boundary condition for the macroscale field.

Compute a basis vector $\vec{\mathbf{w}}$ for the null space of the transpose of the left hand side 4×3 matrix in equation (20):

$$\vec{\mathbf{w}} = \begin{bmatrix} -w_1 (\mathbf{a}_0, \mathbf{a}_1, \mathbf{a}_{0,0}, \mathbf{a}_{0,1}, \mathbf{a}_{1,0}, \mathbf{a}_{1,1}, \mathbf{N}) \\ -(\mathbf{1} - w_1) \\ 1 \\ w_4 (\mathbf{a}_0, \mathbf{a}_1, \mathbf{a}_{0,0}, \mathbf{a}_{0,1}, \mathbf{a}_{1,0}, \mathbf{a}_{1,1}, \mathbf{N}) \end{bmatrix}, \quad (21)$$

where the vector is normalised so that the third component is one. Vector \vec{w} always exists as the matrix in equation (20) is a 4×3 matrix so the null space is never empty. Premultiply (20) by \vec{w}^T to obtain zero on the LHS. Thus the RHS provides the boundary condition at the left end of the domain:

$$\mathbf{U} + w_4 \frac{\partial \mathbf{U}}{\partial x} = w_1 \mathbf{u}_{0,0} + (1 - w_1) \mathbf{u}_{0,1}. \quad (22)$$

This Robin boundary condition generates the accurate macroscale solution in the domain interior of Figure 3.

Computer algebra shows w_4 is a complicated function, but is $\mathcal{O}(1/N)$. Thus for N large the coefficient $w_4 \approx 0$ in the boundary condition (22). The boundary condition then reduces to the classic Dirichlet condition $\mathbf{U} = w_1 \mathbf{u}_{0,0} + (1 - w_1) \mathbf{u}_{0,1}$ (Mei and Vernescu, 2010; Pavliotis and Stuart, 2008).

3.3 Macroscopic boundary conditions at $x = L$

We derive the right macroscopic boundary condition using a similar approach as in Section 3.2. The only modification of the methodology is to interchange the role of \mathbf{c}_1 and \mathbf{c}_4 ¹. The decaying mode coefficient is zero ($\mathbf{c}_1 = 0$) when dealing with the right boundary, otherwise the left boundary value would be exponentially large. We multiply cells by T^{-1} when considering evolution from the right to the left. In the core μ_4^{-n} is negligible. Following the same procedure in Section 3.2, we get the corresponding boundary condition at the right.

¹Another approach is to execute the same spatial analysis on matrix T^{-1} . This corresponds to using a new opposite coordinate system that increases from right to left.

4 Result and conclusion

We ran numerous numerical examples to verify our analytical results. Figure 3 shows one example with $N = 25$. The lateral diffusivities in this example are $\alpha_{0,0} = 0.5$, $\alpha_{0,1} = 0.4$, $\alpha_{1,0} = 0.3$ and $\alpha_{1,1} = 0.1$, whereas the cross diffusivities are smaller at $\alpha_0 = 0.05$ and $\alpha_1 = 0.02$. The microscale boundary conditions are $u_{0,0} = -5$, $u_{0,1} = 0$ at the left end, and $u_{N,0} = -13$, $u_{N,1} = 4$ at the right end. The boundary conditions for this particular case are symmetric

$$u + 0.04 \frac{\partial u}{\partial x} = 0.67u_{n,0} + 0.33u_{n,1}, \quad \text{for } n = 0, N. \quad (23)$$

With these boundary conditions the macroscale solution is not influenced by the boundary layers and produces an accurate fit to the microscale solution within the interior of the domain, thus better describing the global behaviour than the solution with classic boundary conditions (22) with $w_4 = 0$.

The approach developed here is readily modified to more complicated problems such as wave equations and beams with microscale metamaterial structures.

Acknowledgements CC thanks CSIRO for their support in funding to attend conferences and workshops and thanks Tony Miller for his advice. The Australian Research Council Discovery Project grant DP120104260 also helped support this research.

References

- A. Baron, A. Iazzolino, K. Ehrhardt, J.-B. Salmon, A. Aradian, V. Kravets, A. N. Grigorenko, J. Leng, A. Le Beulze, M. Tréguer-Delapierre, M. A. Correa-Duarte, and P. Barois. Bulk optical metamaterials assembled by microfluidic evaporation. *Opt. Mater. Express*, 3(11):1792–1797, 2013. doi:[10.1364/OME.3.001792](https://doi.org/10.1364/OME.3.001792). C220

- J. Carr. Applications of Centre Manifold Theory. *Applied Mathematical Sciences*, 35, 1982. doi:[10.1007/978-1-4612-5929-9](https://doi.org/10.1007/978-1-4612-5929-9) C224
- J. Carr and R. G. Muncaster. The application of centre manifolds to amplitude expansions. I. ordinary differential equations. *J. Differ. Equations*, 50(2):260–279, 1983. doi:[10.1016/0022-0396\(83\)90077-3](https://doi.org/10.1016/0022-0396(83)90077-3). C224
- Y. Dong and T. Itoh. Promising future of metamaterials. *IEEE Microw. Mag.*, 13(2):39–56, 2012. doi:[10.1109/MMM.2011.2181447](https://doi.org/10.1109/MMM.2011.2181447). C220
- G. V. Eleftheriades and M. Selvanayagam. Transforming electromagnetics using metamaterials. *IEEE Microw. Mag.*, 13(2):26–38, 2012. doi:[10.1109/MMM.2011.2181446](https://doi.org/10.1109/MMM.2011.2181446). C220
- C. C. Mei and B. Vernescu. *Homogenization methods for multiscale mechanics*. World Scientific, Hackensack, NJ, 2010. <http://www.worldscientific.com/worldscibooks/10.1142/7427> C220, C231
- G. N. Mercer and A. J. Roberts. A centre manifold description of contaminant dispersion in channels with varying flow properties. *SIAM J. Appl. Math.*, 50(6):1547–1565, 1990. doi:[10.1137/0150091](https://doi.org/10.1137/0150091). C221
- G. A. Pavliotis and A. M. Stuart. *Multiscale Methods: Averaging and Homogenization*. Springer, 2008. <http://www.springer.com/mathematics/dynamical+systems/book/978-0-387-73828-4> C231
- A. J. Roberts. Boundary conditions for approximate differential equations. *J. Aust. Math. Soc.*, 34:54–80, 1992. doi:[10.1017/S0334270000007384](https://doi.org/10.1017/S0334270000007384). C221, C227
- A. J. Roberts. *Model emergent dynamics in complex systems*. August 2011. C221, C224

Author addresses

1. **Chen Chen**, School of Mathematical Sciences, University of Adelaide, South Australia 5005, AUSTRALIA.
<mailto:chen.chen@adelaide.edu.au>
2. **A. J. Roberts**, School of Mathematical Sciences, University of Adelaide, South Australia 5005, AUSTRALIA.
<mailto:anthony.roberts@adelaide.edu.au>
3. **J. E. Bunder**, School of Mathematical Sciences, University of Adelaide, South Australia 5005, AUSTRALIA.
<mailto:judith.bunder@adelaide.edu.au>